

Dynamics of spin-orbital-angular-momentum coupled Bose-Einstein condensates on a ring

Lin Wen(文林), Yi-Han Huang(黄燚寒), Lei Zhao(赵磊), Xu Qiu(邱旭), and Ming-Yue Yang(杨明月)
Citation: Chin. Phys. B, 2026, 35 (**6**): 060305. DOI: 10.1088/1674-1056/ae5b5c
http://cpb.iphy.ac.cn; http://iopscience.iop.org/cpb

What follows is a list of articles you may be interested in

Exceptional rings and non-Abelian topology in non-Hermitian high-spin systems

Peng-Zhen Sun(孙鹏震), Zhou-Tao Lei(雷周涛), and Yuan-Gang Deng(邓元刚)
Chin. Phys. B, 2025, 34 (**11**): 110303. DOI: 10.1088/1674-1056/addcbe

Floquet engineering of a dynamical Z_2 lattice gauge field with ultracold atoms

Xiangxiang Sun(孙祥祥), Hao-Yue Qi(齐浩月), Pengfei Zhang(张鹏飞), and Wei Zheng(郑炜)
Chin. Phys. B, 2024, 33 (**11**): 110304. DOI: 10.1088/1674-1056/ad7576

Observation of flat-band localized state in a one-dimensional diamond momentum lattice of ultracold atoms

Chao Zeng(曾超), Yue-Ran Shi(石悦然), Yi-Yi Mao(毛一屹), Fei-Fei Wu(武菲菲), Yan-Jun Xie(谢岩骏), Tao Yuan(苑涛), Han-Ning Dai(戴汉宁), and Yu-Ao Chen(陈宇翱)
Chin. Phys. B, 2024, 33 (**1**): 010303. DOI: 10.1088/1674-1056/ad0cd1

Atom-pair tunneling and quantum phase transition in asymmetry double-well trap in strong-interaction regime

Ji-Li Liu(刘吉利), Jiu-Qing Liang(梁九卿)
Chin. Phys. B, 2019, 28 (**11**): 110304. DOI: 10.1088/1674-1056/ab44b6

Sonic horizon dynamics of ultracold Fermi system under elongated harmonic potential

Ying Wang(王颖), Shuyu Zhou(周蜀渝)
Chin. Phys. B, 2018, 27 (**10**): 100312. DOI: 10.1088/1674-1056/27/10/100312

Dynamics of spin–orbital-angular-momentum coupled Bose–Einstein condensates on a ring

Lin Wen(文林)[1], Yi-Han Huang(黄燚寒)[1], Lei Zhao(赵磊)[1], Xu Qiu(邱旭)[1,2,†], and Ming-Yue Yang(杨明月)[3,‡]

[1] *College of Physics and Optoelectronic Engineering, Chongqing Normal University, Chongqing* 401331, *China*
[2] *College of Physics and Electronic Engineering, Northwest Normal University, Lanzhou* 730070, *China*
[3] *Department of Physics, Capital Normal University, Beijing* 100048, *China*

(Received 4 February 2026; revised manuscript received 16 March 2026; accepted manuscript online 3 April 2026)

We investigate the dynamics of a two-component Bose–Einstein condensate subject to spin–orbital-angular-momentum coupling and confined to a ring, via the variational approach. Adopting a single-mode approximation by assuming that the BEC carries a single angular momentum for SU(2)-symmetric spin interactions, the equations of motion for the variational parameters are derived. The phase diagram of the ground state in the plane of the Raman coupling and detuning contains three different phases which meet at a tricritical point, and the exact phase boundaries between the three phases are determined. Linear stability analysis shows that the stationary state is dynamically stable, and there exists an oscillation eigenmode with frequency determined by detuning, angular momentum, and Raman coupling. The time-evolution results indicate that the spin vector undergoes periodic rotation along a closed orbit on the Bloch sphere, which can be interpreted as a precession of the collective spin around an effective field determined by the Raman coupling strength, the detuning, and the angular momentum.

Keywords: ultracold atom, Bose–Einstein condensate, spin-orbital–angular-momentum coupling

PACS: 03.75.Mn, 37.10.Vz, 67.85.–d

DOI: 10.1088/1674-1056/ae5b5c **CSTR:** 32038.14.CPB.ae5b5c

1. Introduction

Spin–orbital-angular-momentum coupling describes the interaction between a particle's spin magnetic moment and the effective magnetic field associated with its orbital motion.[1] As a fundamental quantum mechanical effect, it is crucial for understanding atomic structure and the microscopic origin of chemical bonding. In recent years, light–atom interactions in ultracold-atom experiments have enabled the engineering of synthetic gauge fields for neutral atoms, including spin–linear-momentum coupling (SLMC)[2–5] and spin–orbital-angular-momentum coupling (SOAMC).[6–8] These advances make ultracold atomic gases with SLMC or SOAMC a versatile platform for exploring unconventional quantum phases and novel dynamical phenomena.

In ultracold atomic gases with SLMC, the coupling between an atom's internal spin and its center-of-mass momentum gives rise to stripe phases,[9–15] fractional-vortex states,[16–21] and exotic solitonic excitations.[22–29] In contrast, in systems with SOAMC, atoms populate well-defined orbital-angular-momentum states, so the condensate wave function naturally carries a nonzero winding number, enabling unconventional quantum phases that are absent in more conventional ultracold gases, most notably angular stripe states.[30–39]

To the best of our knowledge, previous studies on Bose–Einstein condensates (BECs) with SOAMC have mainly focused on identifying novel ground states, whereas their dynamical properties, especially the real-time evolution and linear stability, have received much less attention. In such systems, the atomic spin is coupled to the quantized orbital angular momentum associated with the circulation of the BEC. Consequently, the atomic spin dynamics and the orbital motion are no longer independent but are intrinsically intertwined. It is therefore natural to expect that SOAMC can significantly affect the dynamical behavior of the BEC, including its spin dynamics, dynamical stability, and low-energy excitation modes. Exploring these issues can provide a deeper understanding of the dynamical consequences of SOAMC in BECs.

In this work, we focus on a two-component BEC with SOAMC confined to a ring and study both its ground state and its real-time dynamics along the azimuthal direction. Starting from a single-particle Hamiltonian with SOAMC generated by two Laguerre–Gaussian (LG) Raman beams, we derive an effective one-dimensional mean-field model on the ring. Adopting a single-mode approximation by assuming that the BEC carries a single angular momentum for SU(2)-symmetric spin interactions, and using the variational method, we obtain equations of motion for the variational parameters and map out the ground-state phase diagram in the plane of Raman coupling and detuning, together with the exact phase boundaries; a tri-

†Corresponding author. E-mail: xuqiu@cqnu.edu.edu
‡Corresponding author. E-mail: 2220601001@cnu.edu.cn

© 2026 Chinese Physical Society and IOP Publishing Ltd. All rights, including for text and data mining, AI training, and similar technologies, are reserved.

critical point in the phase diagram is identified. We further perform a linear-stability analysis around the stationary state and find that the stationary state is dynamically stable, and there exists an oscillation eigenmode with frequency determined by detuning, angular momenta, and Raman coupling. Finally, we obtain the exact full dynamical solutions of the variational parameters, revealing that the spin vector undergoes periodic rotation along a closed orbit on the Bloch sphere.

2. Model

We consider a two-component BEC coupled by a pair of copropagating LG Raman beams. The Raman process transfers the orbital angular momenta of the LG beams to the two spin states and realizes SOAMC. In cylindrical coordinates, the corresponding single-particle Hamiltonian reads[6–8]

$$\begin{aligned}\hat{H}_0 =& -\frac{\hbar^2}{2M}\frac{1}{r}\frac{\partial}{\partial r}\left(r\frac{\partial}{\partial r}\right)+\frac{\left(\hat{L}_z-l\hbar\sigma_z\right)^2}{2Mr^2}\\&+\Omega_{\mathrm{R}}(r)\sigma_x+\frac{\Delta}{2}\sigma_z,\end{aligned}\tag{1}$$

where r is the radius, θ is the azimuthal angle, M is the atomic mass, $\hat{L}_z=-\mathrm{i}\hbar\partial_\theta$ is the z component of the angular momentum operator. $\Omega_{\mathrm{R}}=I(r/w)^{|l_1|+|l_2|}\,\mathrm{e}^{-2r^2/w^2}$ represents the spatially dependent Raman coupling with I being the coupling strength, and w is the waist of the beams, l_1 and l_2 are the angular momenta of the two lasers, and $l=(l_1-l_2)/2$. $\sigma_{x,z}$ is the Pauli matrix, and Δ is the two-photon detuning.

We assume the BEC is confined on a uniform ring with radius R so that the system is effectively one-dimensional along the azimuth angle θ, and consider the SU(2)-symmetric spin interactions by taking all interaction strengths to be equal to a single value g. Measuring energy in units of $E_{\mathrm{R}}=\hbar^2/(MR^2)$ and time in units of $\hbar/E_{\mathrm{R}}$, and defining the dimensionless parameters $\Omega=\Omega_{\mathrm{R}}(R)/E_{\mathrm{R}}$ and $\delta=\Delta/E_{\mathrm{R}}$, the mean-field dynamics of the BEC at zero temperature can be governed by the dimensionless Gross–Pitaevskii (GP) equation

$$\mathrm{i}\frac{\partial\psi_\uparrow}{\partial t}=\frac{1}{2}\left(-\mathrm{i}\frac{\partial}{\partial\theta}-l\right)^2\psi_\uparrow+\Omega\psi_\downarrow+\frac{\delta}{2}\psi_\uparrow+g\rho\,\psi_\uparrow,\tag{2a}$$

$$\mathrm{i}\frac{\partial\psi_\downarrow}{\partial t}=\frac{1}{2}\left(-\mathrm{i}\frac{\partial}{\partial\theta}+l\right)^2\psi_\downarrow+\Omega\psi_\uparrow-\frac{\delta}{2}\psi_\downarrow+g\rho\,\psi_\downarrow,\tag{2b}$$

where $\rho=|\psi_\uparrow|^2+|\psi_\downarrow|^2$ is the total density satisfying the normalization condition $\int_0^{2\pi}\rho(\theta)\mathrm{d}\theta=1$, and g denotes the effective one-dimensional interaction strength on the ring. The corresponding energy functional is

$$\begin{aligned}\mathcal{E}=&\int_0^{2\pi}\mathrm{d}\theta\left\{\Psi^\dagger\left[\frac{1}{2}\left(-\mathrm{i}\frac{\partial}{\partial\theta}-l\sigma_z\right)^2+\Omega\sigma_x+\frac{\delta}{2}\sigma_z\right]\Psi\right.\\&\left.+\frac{g}{2}\left(\Psi^\dagger\Psi\right)^2\right\}.\end{aligned}\tag{3}$$

In this paper, we focus on the case with $l=1$; the same analysis can also be readily generalized to $l>1$.

3. Theoretical method

To develop an analytical analysis, we employ a variational approximation to investigate the dynamics of the system,[40] based on the Lagrangian

$$\mathcal{L}=\int_0^{2\pi}\frac{\mathrm{i}}{2}\left(\Psi^\dagger\frac{\partial\Psi}{\partial t}-\frac{\partial\Psi^\dagger}{\partial t}\Psi\right)\mathrm{d}\theta-\mathcal{E},\tag{4}$$

where $\Psi(\theta,t)=\left[\psi_\uparrow(\theta,t),\psi_\downarrow(\theta,t)\right]^{\mathrm{T}}$ with T being the transpose. We adopt a single-mode approximation by assuming that the BEC carries a single angular momentum due to SOAMC, and thus take the condensate wave functions as

$$\Psi(\theta,t)=\frac{\mathrm{e}^{\mathrm{i}m\theta}}{\sqrt{2\pi}}\begin{pmatrix}\sin\alpha(t)\,\mathrm{e}^{\mathrm{i}\varphi_\uparrow(t)}\\\cos\alpha(t)\,\mathrm{e}^{\mathrm{i}\varphi_\downarrow(t)}\end{pmatrix},\tag{5}$$

where the integer m is the angular momentum or winding number, which is conserved due to the rotation symmetry. Physically, α controls the relative weight of the two spin components, while $\varphi_\uparrow$ and $\varphi_\downarrow$ represent the phases of the two wave functions. Without loss of generality, α, $\varphi_\uparrow$, and $\varphi_\downarrow$ are time-dependent variational parameters. It should be pointed out that this single-mode approximation is reliable for a uniform ring and the SU(2)-symmetric spin interactions considered in this work. In contrast, asymmetric spin interactions and/or nonuniform trapping may induce substantial mixing between different angular-momentum modes; hence, multimode superpositions may become important and lead to angular-density modulation or more complicated spin textures.[30–39]

Defining $\varphi_\pm=\varphi_\uparrow\pm\varphi_\downarrow$, insertion of Eq. (5) into Eq. (3) gives

$$\begin{aligned}\mathcal{E}=&\,\Omega\sin(2\alpha)\cos(\varphi_-)+\left(m-\frac{\delta}{2}\right)\cos(2\alpha)\\&+\frac{1}{2}\left(m^2+1\right)+\frac{g}{4\pi},\end{aligned}\tag{6}$$

and the reduced Lagrangian

$$\mathcal{L}=-\frac{1}{2}\dot{\varphi}_+-\frac{1}{2}\cos(2\alpha)\dot{\varphi}_--\mathcal{E}.\tag{7}$$

The equations of motion for the variational parameters can be obtained from the Euler–Lagrange equation $\frac{\partial\mathcal{L}}{\partial A}-\frac{\mathrm{d}}{\mathrm{d}t}\left(\frac{\partial\mathcal{L}}{\partial\dot{A}}\right)=0$ (where A is a variational parameter and $\dot{A}=\frac{\mathrm{d}A}{\mathrm{d}t}$):

$$\dot{\alpha}=-\Omega\sin(\varphi_-),\tag{8a}$$

$$\dot{\varphi}_-=-2\Omega\cot(2\alpha)\cos(\varphi_-)+2m-\delta.\tag{8b}$$

Obviously, α and φ_- are coupled nonlinearly by the Raman coupling, angular momentum, and detuning, so the BEC would display interesting dynamics. However, φ_+ decouples from the other variational parameters and makes no contribution to the dynamics. Moreover, it should be emphasized that the interaction term enters the Lagrangian Eq. (7) only as

a constant due to the SU(2)-symmetric spin interactions under the single-mode approximation. Therefore, the equations of motion are independent of the interaction parameters. For asymmetric interactions or multimode states with nonuniform density, the nonlinear term would, in general, modify the equations of motion and affect the dynamics of the BEC.

To further clarify the underlying physics behind SOAMC, we introduce the spatially averaged spin $S_j = \int_0^{2\pi} \Psi^\dagger \sigma_j \Psi \, \mathrm{d}\theta$ ($j = x, y, z$). With the wave function (5), the spin becomes

$$\begin{pmatrix} S_x \\ S_y \\ S_z \end{pmatrix} = \begin{pmatrix} \sin(2\alpha)\cos(\varphi_-) \\ -\sin(2\alpha)\sin(\varphi_-) \\ -\cos(2\alpha) \end{pmatrix}. \tag{9}$$

Using Eqs. (8a) and (8b), one obtains the equations of motion of the spin

$$\dot{S}_x = (2m-\delta)S_y, \tag{10a}$$

$$\dot{S}_y = -2\Omega S_z - (2m-\delta)S_x, \tag{10b}$$

$$\dot{S}_z = 2\Omega S_y. \tag{10c}$$

These equations of motion for the spin can also be rewritten as the form $\dot{\boldsymbol{S}} = \boldsymbol{B} \times \boldsymbol{S}$ with $\boldsymbol{B} = (2\Omega, 0, \delta - 2m)$, which represents the Bloch equation for the spin precession under the action of the effective field $\boldsymbol{B}$. It is worth emphasizing that the appearance of the angular momentum m in the effective field $\boldsymbol{B}$ shows that the spin dynamics is also influenced by the angular momentum, which is a direct manifestation of SOAMC.

4. Results and discussion

We first analyze the properties of the stationary state, where the variational parameters α and φ_- are time independent. The stationarity condition $\dot{\alpha} = 0$ in Eq. (8a) yields $\sin(\varphi_-) = 0$, *i.e.*, $\varphi_- = 0$, or π. For $\Omega \geq 0$, if we restrict $\alpha \in \left[0, \frac{\pi}{2}\right]$, the energy can be minimized by choosing $\varphi_- = \pi$, which gives $\cos\varphi_- = -1$ and aligns the transverse spin S_x antiparallel to the effective transverse $B_x = 2\Omega$. In this case, Eq. (8b) becomes

$$\tan(2\alpha) = \frac{2\Omega}{\delta - 2m}. \tag{11}$$

Equation (11) makes it explicit that for $|\delta - 2m| \gg \Omega$ the BEC is nearly polarized due to $\alpha \sim 0$, while for $\delta \approx 2m$ the two components are population balanced due to $\alpha \sim \frac{\pi}{4}$.

Eliminating α and φ_- from the energy functional yields

$$\mathcal{E}(m) = \frac{1}{2}\left(m^2+1\right) - \frac{1}{2}\sqrt{4\Omega^2 + (2m-\delta)^2} + \frac{g}{4\pi}, \tag{12}$$

which is an effective energy functional depending only on m for fixed δ, Ω, and g. In Eq. (12), the first term represents the kinetic cost due to the angular momentum, while the square-root term is the lower dressed-state energy resulting from the competition between Raman coupling and the effective longitudinal field $B_z = 2m - \delta$. The m-dependent energy dispersion $\mathcal{E}(m)$ is shown in Fig. 1. For $\delta = 0$, the energy is invariant under the reflection transformation $\theta \to -\theta$, *i.e.*, $\mathcal{E}(m) = \mathcal{E}(-m)$. Therefore, the states with m and $-m$ are twofold degenerate, and the dispersion is mirror-symmetric about $m = 0$, as shown in Fig. 1(a). For $\delta \neq 0$, the reflection symmetry is broken and the degeneracy between $\pm m$ is lifted, as shown in Fig. 1(b).

For the ground state, the angular momentum can be determined by solving the stationary-condition equation $\frac{\partial \mathcal{E}}{\partial m} = 0$ under the condition that $\frac{\partial^2 \mathcal{E}}{\partial m^2} > 0$. If m is temporarily regarded as a continuous variable, one can first identify the corresponding minimizer m^* of the energy. Since m is in fact

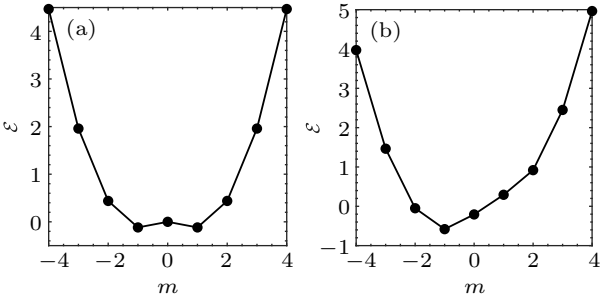


Fig. 1. (a) and (b) The energy dispersion curves for $\delta = 0$ and $\delta = 1$, respectively. The parameter $\Omega = 0.5$.

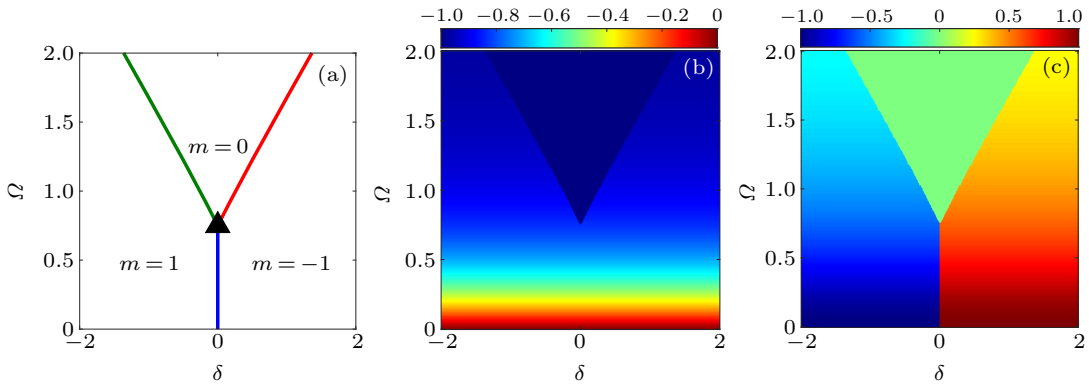


Fig. 2. (a) The phase diagram of the ground state in the plane of Ω and δ, where the blue, red, and green solid lines are the phase boundaries $\delta = 0$, $\Omega = \sqrt{\frac{3}{16}(2\delta+3)(2\delta+1)}$, and $\Omega = \sqrt{\frac{3}{16}(2\delta-3)(2\delta-1)}$, respectively. The black solid triangle marks the tricritical point; panels (b) and (c) show the evolutions of S_x and S_z with Ω and δ in the ground state, respectively.

restricted to integer values, however, the actual ground state is selected not by m^* itself, but from the nearest integers around m^*. Figure 2(a) presents the ground-state phase diagram in the (Ω,δ) plane, which contains three different phases characterized by $m=-1$, 0, and $+1$, corresponding to different angular momenta. The phase boundaries between phases can be determined by equating their energies. Specifically, the phase boundary between the $m=+1$ and $m=-1$ phases is $\delta=0$, the phase boundary between the $m=-1$ and $m=0$ phases is $\Omega=\sqrt{\frac{3}{16}(2\delta+3)(2\delta+1)}$, and the phase boundary between the $m=+1$ and $m=0$ phases is $\Omega=\sqrt{\frac{3}{16}(2\delta-3)(2\delta-1)}$. In particular, a tricritical point occurs at $\delta=0$ and $\Omega=3/4$, where the three phases meet and become degenerate; hence the location of the tricritical point in the phase diagram is determined by the condition $\mathcal{E}(m=0)=\mathcal{E}(m=+1)=\mathcal{E}(m=-1)$. Furthermore, Figs. 2(b) and 2(c) show the ground-state spin components S_x and S_z in the (Ω,δ) plane. In the $m=0$ phase, $(S_x,S_y,S_z)=(-1,0,0)$ indicates that the BEC is fully spin-polarized along the negative x direction. In the $m=+1$ and $m=-1$ phases, they have opposite angular momentum and S_z; the absolute values of both S_x and S_z are smaller than 1.

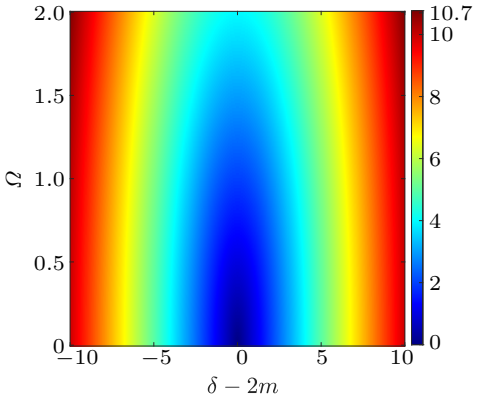


Fig. 3. The frequency $|\omega|$ as a function of $\delta-2m$ and Ω.

To proceed, we assess the stability of the stationary state against a small perturbation. Setting $\alpha(t)=\alpha_*+\tilde{\alpha}(t)$ and $\varphi_-(t)=\varphi_{-,*}+\tilde{\varphi}_-(t)$, where α_* and $\varphi_{-,*}$ represent the stationary state solutions solved from Eq. (8) by setting $\frac{\mathrm{d}\alpha}{\mathrm{d}t}=\frac{\mathrm{d}\varphi_-}{\mathrm{d}t}=0$, $\tilde{\alpha}(t)$ and $\tilde{\varphi}_-(t)$ denote the small time-dependent departures from the stationary state solutions under a small perturbation. Linearizing Eq. (8) results in the following ordinary differential equations:

$$\frac{\mathrm{d}}{\mathrm{d}t}\begin{pmatrix}\tilde{\alpha}\\ \tilde{\varphi}_-\end{pmatrix}=\begin{pmatrix}0 & \Omega\\ -\frac{4\Omega}{\sin^2(2\alpha_*)} & 0\end{pmatrix}\begin{pmatrix}\tilde{\alpha}\\ \tilde{\varphi}_-\end{pmatrix}. \tag{13}$$

The corresponding eigenfrequencies are

$$\omega=\pm\sqrt{(\delta-2m)^2+4\Omega^2}, \tag{14}$$

which are purely real for all parameters, implying that the stationary state is therefore dynamically stable and a small perturbation generates a periodic oscillation with frequency $|\omega|$. As shown in Fig. 3, the frequency $|\omega|$ increases with both $|\delta-2m|$ and Ω, and vanishes only at $\delta=2m$ and $\Omega=0$. Experimentally, this frequency can be extracted from the oscillation period of the spin-resolved populations after a quench of either Ω or δ.

Finally, we investigate the real-time dynamics of BEC on a ring. Since the BEC is rotation-invariant, the angular momenta are conserved. Therefore, the motion equation (10) of the spin can be solved exactly:

$$S_x(t) = \frac{4\Omega^2S_{x,0}-2\Omega\zeta S_{z,0}}{\omega^2}+\frac{\zeta^2S_{x,0}+2\Omega\zeta S_{z,0}}{\omega^2}\cos(\omega t) + \frac{\zeta S_{y,0}}{\omega}\sin(\omega t), \tag{15a}$$

$$S_y(t) = S_{y,0}\cos(\omega t)-\frac{\zeta S_{x,0}+2\Omega S_{z,0}}{\omega}\sin(\omega t), \tag{15b}$$

$$S_z(t) = \frac{\zeta^2S_{z,0}-2\Omega\zeta S_{x,0}}{\omega^2}+\frac{2\Omega\zeta S_{x,0}+4\Omega^2S_{z,0}}{\omega^2}\cos(\omega t) + \frac{2\Omega S_{y,0}}{\omega}\sin(\omega t), \tag{15c}$$

where $\zeta=2m-\delta$. These expressions make explicit that the spin would oscillate periodically with frequency ω and that the dynamics is fully controlled by the detuning δ, angular momenta m, and the Raman coupling Ω. In particular, if $\delta=2m$, then the oscillation frequency is determined completely by the Raman coupling. Moreover, from Eq. (9), the exact solutions of $\alpha(t)$ and $\varphi_-(t)$ can also be obtained immediately:

$$\alpha(t)=\frac{1}{2}\arccos(-S_z),\quad \varphi_-(t)=\arctan\left(-\frac{S_y}{S_x}\right). \tag{16}$$

As a typical example, Fig. 4 illustrates the spin oscillation for the initial-polarized state $\boldsymbol{S}(0)=(0,0,1)$, where $S_x(t)=-\frac{4\Omega\zeta}{\omega^2}\sin^2\left(\frac{\omega}{2}t\right)$, $S_y(t)=-\frac{2\Omega}{\omega}\sin(\omega t)$, and $S_z(t)=\frac{\zeta^2}{\omega^2}+\frac{4\Omega^2}{\omega^2}\cos(\omega t)$, the spin vector $\boldsymbol{S}$ rotates periodically along a closed orbit on the Bloch sphere.

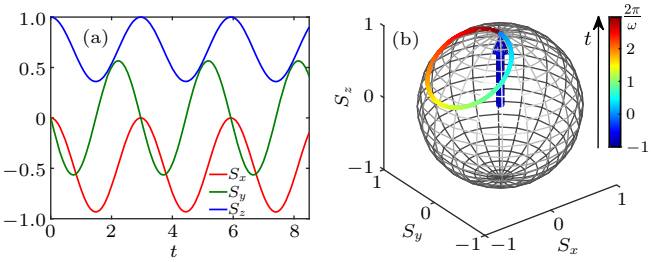


Fig. 4. (a) Time evolution of the spin components S_x, S_y, S_z; (b) trajectory of $\boldsymbol{S}(t)$ on the Bloch sphere. The blue arrow represents the spin vector at $t=0$. The colored line is the trajectory of the spin vector, and the colorbar is the corresponding time. The parameters in panels (a) and (b) are $\Omega=0.6$, $m=1$, and $\delta=0.25$.

The predicted spin dynamics can be probed experimentally through the time evolution of the spin-resolved populations or the averaged spin components. Conversely, because the spin degree of freedom is coupled to the orbital angular momentum in the presence of SOAMC, the observed spin dynamics can also provide information about

the angular momentum of the BEC. Therefore, the present model predicts not only spin precession but also an angular-momentum-dependent spin dynamics characteristic of a BEC with SOAMC.

5. Conclusion

In this paper, we study the dynamics of a two-component BEC with SOAMC. By assuming the BEC is confined to a ring, we derive an effective one-dimensional mean-field model along the azimuthal angle and use the variational method to obtain the equations of motion for the variational parameters. In the plane of Raman coupling and detuning, we depict the phase diagram of the ground state, which contains three different phases. The three phases meet at a tricritical point, and the exact phase boundaries among them are established. By further performing a linear stability analysis around the ground state under perturbation, we find the ground state is dynamically stable, and there exists an oscillation eigenmode with a frequency related to the detuning, angular momenta, and Raman coupling. Finally, we obtain the exact full dynamical solutions of the variational parameters, which show that the spin vector rotates periodically along a closed orbit on a Bloch sphere.

Acknowledgements

Project by the National Natural Science Foundation of China (Grant Nos. 12175027 and 11875010), the Natural Science Foundation of Chongqing (Grant No. CSTB2025NSCQ-GPX1010), and the Science and Technology Research Program of Chongqing Municipal Education Commission (Grant No. KJQN202500531).

References

[1] Sakurai J J and Napolitano J 2020 *Modern Quantum Mechanics*, 3rd end. (Cambridge University Press)
[2] Lin Y J, Jiménez-García K and Spielman I B 2011 *Nature* **471** 83
[3] Zhang J Y, Ji S C, Chen Z, Zhang L, Du Z D, Yan B, Pan G S, Zhao B, Deng Y J, Zhai H, Chen S and Pan J W 2012 *Phys. Rev. Lett.* **109** 115301
[4] Wang P, Yu Z Q, Fu Z, Miao J, Huang L, Chai S, Zhai H and Zhang J 2012 *Phys. Rev. Lett.* **109** 095301
[5] Cheuk L W, Sommer A T, Hadzibabic Z, Yefsah T, Bakr W S and Zwierlein M W 2012 *Phys. Rev. Lett.* **109** 095302
[6] Chen H R, Lin K Y, Chen P K, Chiu N C, Wang J B, Chen C A, Huang P P, Yip S K, Kawaguchi Y and Lin Y J 2018 *Phys. Rev. Lett.* **121** 113204
[7] Chen P K, Liu L R, Tsai M J, Chiu N C, Kawaguchi Y, Yip S K, Chang M S and Lin Y J 2018 *Phys. Rev. Lett.* **121** 250401
[8] Zhang D, Gao T, Zou P, Kong L, Li R, Shen X, Chen X L, Peng S G, Zhan M, Pu H and Jiang K 2019 *Phys. Rev. Lett.* **122** 110402
[9] Wang C, Gao C, Jian C M and Zhai H 2010 *Phys. Rev. Lett.* **105** 160403
[10] Ho T L and Zhang S 2011 *Phys. Rev. Lett.* **107** 150403
[11] Zhang Y, Mao L and Zhang C 2012 *Phys. Rev. Lett.* **108** 035302
[12] Li Y, Pitaevskii L P and Stringari S 2012 *Phys. Rev. Lett.* **108** 225301
[13] Wen L, Sun Q, Wang H Q, Ji A C and Liu W M 2012 *Phys. Rev. A* **86** 043602
[14] Sun Q, Wen L, Liu W M, Juzeliunas G and Ji A C 2015 *Phys. Rev. A* **91** 033619
[15] Su S W, Gou S C, Sun Q, Wen L, Liu W M, Ji A C, Ruseckas J and Juzeliunas G 2016 *Phys. Rev. A* **93** 053630
[16] Sinha S, Nath R and Santos L 2011 *Phys. Rev. Lett.* **107** 270401
[17] Hu H, Ramachandhran B, Pu H and Liu X J 2012 *Phys. Rev. Lett.* **108** 010402
[18] Kawakami T, Mizushima T, Nitta M and Machida K 2012 *Phys. Rev. Lett.* **109** 015301
[19] Wilson R M, Anderson B M and Clark C W 2013 *Phys. Rev. Lett.* **111** 185303
[20] Liu C F, Wan W J and Zhang G Y 2013 *Acta Phys. Sin.* **62** 200306 (in Chinese)
[21] Li J, Liu B, Bai J, Wang H Y and He T C 2020 *Acta Phys. Sin.* **69** 140301 (in Chinese)
[22] Wang Y, Cui J, Zhang H, Zhao Y, Xu S and Zhou Q 2024 *Chin. Phys. Lett.* **41** 090302
[23] He J T, Fang P P and Lin J 2022 *Chin. Phys. Lett.* **39** 020301
[24] Guo H, Qiu X, Ma Y, Jiang H F and Zhang X F 2021 *Chin. Phys. B* **30** 060310
[25] Xu Y, Zhang Y and Wu B 2013 *Phys. Rev. A* **87** 013614
[26] Achilleos V, Frantzeskakis D J, Kevrekidis P G and Pelinovsky D E 2013 *Phys. Rev. Lett.* **110** 264101
[27] Kartashov Y V, Konotop V V and Abdullaev F K 2013 *Phys. Rev. Lett.* **111** 060402
[28] Zhang Y, Xu Y and Busch T 2015 *Phys. Rev. A* **91** 043629
[29] Wen L, Sun Q, Chen Y, Wang D S, Hu J, Chen H, Liu W M, Juzeliunas G, Malomed B A and Ji A C 2016 *Phys. Rev. A* **94** 061602
[30] Duan Y, Bidasyuk Y M and Surzhykov A 2021 *Phys. Rev. A* **102** 063328
[31] Chen K J, Wu F, Peng S G, Yi W and He L Y 2020 *Phys. Rev. Lett.* **125** 260407
[32] Wang L L, Ji A C, Sun Q and Li J 2021 *Phys. Rev. Lett.* **126** 193401
[33] Edmonds M 2021 *Phys. Rev. A* **104** 043310
[34] Bidasyuk Y M, Kovtunenko K S and Prikhodko O O 2022 *Phys. Rev. A* **105** 023320
[35] Cao R, Han J S, Wu J H, Yuan J M, He L Y and Li Y Q 2022 *Phys. Rev. A* **105** 063308
[36] Chen K J, Wu F, Hu J and He L 2020 *Phys. Rev. A* **102** 013316
[37] Chen X L, Peng S G, Zou P and Hu H 2020 *Phys. Rev. Res.* **2** 033152
[38] Sun K, Qu C L and Zhang C W 2015 *Phys. Rev. A* **91** 063627
[39] Chen L, Pu H and Zhang Y B 2016 *Phys. Rev. A* **96** 013629
[40] Malomed B A 2022 *Prog. Opt.* **43** 71